POLITECNICO DI TORINO
Repository ISTITUZIONALE

Softwarized and Autonomous Raman Amplifiers in Multi-Band Open Optical Networks

Original
Softwarized and Autonomous Raman Amplifiers in Multi-Band Open Optical Networks / Borraccini, Giacomo; Ferrari, Alessio; Straullu, Stefano; Nespola, Antonino; D'Amico, Andrea; Piciaccia, Stefano; Galimberti, Gabriele; Tanzi, Alberto; Turolla, Silvia; Curri, Vittorio. - ELETTRONICO. - (2020), pp. 1-6. ((Intervento presentato al convegno International Conference on Optical Network Design and Modelling (ONDM 2020) tenutosi a Castelldefels, Barcelona, Spain nel May 18 –21, 2020 [10.23919/ONDM48393.2020.9133036].

Availability:
This version is available at: 11583/2839536 since: 2020-12-13T10:03:56Z

Publisher:
IEEE

Published
DOI:10.23919/ONDM48393.2020.9133036

Terms of use:
openAccess

This article is made available under terms and conditions as specified in the corresponding bibliographic description in the repository

Publisher copyright
IEEE postprint/Author's Accepted Manuscript

©2020 IEEE. Personal use of this material is permitted. Permission from IEEE must be obtained for all other uses, in any current or future media, including reprinting/republishing this material for advertising or promotional purposes, creating new collecting works, for resale or lists, or reuse of any copyrighted component of this work in other works.

(Article begins on next page)

01 February 2023

Softwarized and Autonomous Raman Amplifiers in Multi-Band Open Optical Networks

Giacomo Borraccini*[(1)], Alessio Ferrari[(1)], Stefano Straullu[(2)], Antonino Nespola[(2)], Andrea D'Amico[(1)], Stefano Piciaccia[(3)], Gabriele Galimberti[(3)], Alberto Tanzi[(3)], Silvia Turolla[(3)], Vittorio Curri[(1)]

[(1)] *Politecnico di Torino, Turin, Italy;* [(2)] *LINKS foundation, Turin, Italy;* [(3)] *Cisco Photonics, Vimercate, Italy*
**giacomo.borraccini@polito.it*

***Abstract*—Starting from the software-defined-network (SDN) concept, this work aims to describe a softwarized system that is able to autonomously design and control Raman amplification in a specific fiber span link. The conceived software module produces the optimum Raman pump power configuration, satisfying amplification constraints given by the control plane through the Raman design unit (RDU). Raman pump power levels are changed using the Raman control Unit (RCU); the initial configuration is generated by the RDU and subsequently used by the RCU to track the mean target gain, according to feedback-provided telemetry data, in order to exploit a linearization of the problem around the optimum solution. This proposal is then validated through an experimental campaign to emulate the *in-field* operation of the system.**

***Index Terms*—Raman amplification, optical communications, optical fiber, multi-band transmission**

I. Introduction

Since the early 2000s, research on Raman amplification in the field of optical communications has become well established, following the largely widespread adoption of the Erbium-doped fiber amplification (EDFA) process [1]. Interest in this process continues to rise as it imparts multiple benefits over traditional amplification methods. Firstly, quality of transmission may be increased via a reduction in noise contributions, improving the equivalent noise figure of the amplification sites [1]–[3]. It also becomes possible to enable long-haul, multi-band transmission [4]–[6] techniques, provided that proper transmission line optimization [7] is performed. Moreover, Raman amplification may also permit a significant increase in the number of available channels. Beyond this, hybrid amplifiers have also been designed – these devices combine both Raman pumps and Erbium doped amplifiers, known as Erbium-doped Raman amplifiers (EDRAs), allowing a high level of amplification to be reached and generating conditions for high-capacity and long-haul transmissions [8]–[10]. In [11]–[13], the authors address the mathematical problem of optimizing Raman amplification working on different gain features and system performance. Furthermore, in [14]–[17] Raman amplification is strongly advised in software-defined-networks (SDNs) to maximize the system performance also in presence of multi-band systems but the specific problem of Raman optimization is not addressed. This work covers the gap by examining the Raman amplification in view of a SDN context, defining a software module able to autonomously handle Raman amplification for a fiber span. In particular, a numerical optimizer is developed in order to find the Raman pump power configuration that matches the required gain constraints for a given fiber span. The structure of such software component is shown, highlighting parameters, variables and metrics upon which it depends. Following this, a possible context is proposed, highlighting the potentialities of the tool through the design of a specific architecture of an embedded controller. Finally, an experimental session has been carried out in order to validate the entire structure and to demonstrate the capability of the softwarized Raman amplification module in emulating in-site operation.

II. Raman Amplification Optimizer

In this section, the numerical tool used to optimize Raman amplification is described, with the goal of defining and clarifying all steps taken to produce the optimal Raman pump power configuration.

A. Physical Model

The distributed Raman amplification on the channel spectrum originates from optical power provided by high frequency lasers, known as pumps, which are used to recover some of the power that is lost during propagation.

The stimulated Raman scattering (SRS) phenomenon is emulated through a system of ordinary differential equations (ODEs) describing the power evolution $P(f_i, z)$ of channels and pumps [1]:

$$\begin{cases} \pm\frac{dP(f_1,z)}{dz} = & -\alpha(f_1)P(f_1,z) + \\ & \sum_{j=2}^{N} C_r(f_1,f_n)P(f_j,z)P(f_1,z) \\ & \dots \\ \pm\frac{dP(f_i,z)}{dz} = & -\alpha(f_i)P(f_i,z) + \\ & \sum_{j=i+1}^{N} C_r(f_i,f_n)P(f_j,z)P(f_i,z) - \\ & \sum_{j=1}^{i-1} \frac{f_i}{f_j} C_r(f_i,f_n)P(f_j,z)P(f_i,z) \\ & \dots \\ \pm\frac{dP(f_N,z)}{dz} = & -\alpha(f_i)P(f_N,z) - \\ & \sum_{j=1}^{N-1} \frac{f_N}{f_j} C_r(f_i,f_n)P(f_j,z)P(f_N,z) \end{cases} \tag{1}$$

where z represents the spatial position along the fiber, $\alpha(f_i)$ is the loss coefficient at the frequency f_i and $C_r(f_i, f_n)$ is the Raman gain efficiency between the frequencies f_i and f_n, where f_1 and f_N are the lower and the higher frequencies, respectively. The sign "$\pm$" gives two cases; one for the signal being co-propagating (+) and one for counter-propagation

(-). Since in this work we treat cases with only counter-propagating pumps, the boundary condition is: $P(f_i, 0)$ for channels and $P(f_i, L_S)$ for pumps, where L_S is the length of the fiber span. The solution is found numerically through successive approximations exploiting the Runge-Kutta method.

In this study, Non-Linear Interference (NLI) generation is not considered. Although in the present derivation Raman amplified spontaneous emission (ASE) is not taken into account, a separation of the noise generated by the Raman effect and by NLI can be considered if a moderate pumping regime is assumed [18].

B. Problem Formulation and Optimization Algorithm

In order to address the optimization problem, the following input parameters must be fixed in advance:

- **Fiber parameters**:
  - Fiber span length L_S
  - Loss coefficient function α;
  - Raman efficiency curve C_r;
  - Concentrated losses along the fiber l_c
- **Spectrum parameters**:
  Channels which represent the input spectrum:
  - Central frequency of each channel f_{ch};
- **Raman pump parameters**:
  Set of Raman pumps:
  - List of Raman pump frequencies f_p;
  - List of Raman pump propagation directions (co-propagating or counter-propagating);
- **ODE solver settings**:
  - Resolution along z axis;
  - Convergence tolerance.

In the case under investigation, the optimization problem can be formulated as follows:

$$\min_x f(x)$$

subject to:

$$c(x) = 0, \quad c(x) \geq 0, \quad lb_i \leq x_i \leq ub_i$$

where $f(x)$ is the objective function, $c(x)$ is the set of equality or inequality constraints and lb_i and ub_i are the lower and upper bounds of the i-th variable to optimize. Raman amplification is defined when the power level and the frequencies are established for each Raman pump. In the use case considered in the present work, the aim is to optimize a set of Raman pump power levels, with pump frequencies fixed in advance.

Assuming a set of N_{RP} Raman pumps, in order to find an optimal solution which can be valid in realistic scenarios, the following bounds and constraint on input variables are imposed:

- **Bounds on pump powers**:
  $0 \leq P_{p,i} \leq 0.5\,W, \quad i = 1, 2, \cdots, N_{RP}$
- **Constraint on maximum total pump power**:
  $\sum_{i=1}^{N_{RP}} P_{p,i} \leq 1.2\,W$

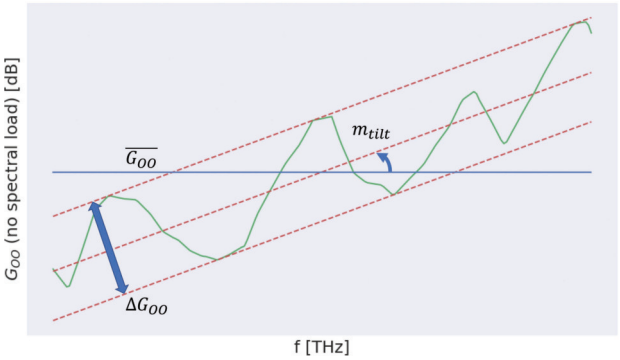

Fig. 1. Metrics of interest in the on-off gain profile $G_{OO}(f_{ch})$.

The optimization algorithm comes from a SciPy library package called *scipy.optimize* [19]. The optimization problem presents a constrained multi-variable nonlinear function. In this framework, the adopted minimization method is the sequential least squares programming algorithm (SLSQP).

C. Objective function

During the research of the optimal solution, the on-off gain profile is computed at each function evaluation. In the optimization procedure, only the depletion mechanism among pumps is considered while pumps vs. channels and inter-channel interactions are neglected, since the amplifiers' working point does not depend *a priori* on the spectral load. Depletion effects related to channels are compensated in a second phase by adjusting the configuration built during the design. The on-off gain profile $G_{OO}(f_{ch})$ obtained by a single pump-channel pair is computed using the formula:

$$G_{OO}(f_{ch}) = \exp\left(\int_0^{L_S} C_r(f_{ch}, f_p) P(f_p, \zeta)\, d\zeta\right) \quad (2)$$

where $C_r(f_{ch}, f_p)$ is the Raman efficiency between the channel and the pump, $P(f_p, \zeta)$ is the pump power spatial evolution. The contribution of each pump is considered analytically identical and so the overall Raman effect on a single channel is equal to the sum of each pump contribution.

After the on-off gain profile computation, the mean value $\overline{G_{OO}}$, the angular coefficient of the linear regression m_{tilt} and the maximum deviation from the linear regression ΔG_{OO} are derived (Fig. 1). Thereby, the objective function is:

$$f(x) = \Delta G_{OO} + |\,\overline{G_{OO}} - \overline{G_{OO,target}}\,| + |\,m_{tilt} - m_{target}\,| \quad (3)$$

where $\overline{G_{OO,target}}$ is the mean on-off gain target value and m_{target} is the tilt target value. These target values are necessary requirements of the numerical optimizer in order to uniquely define the characteristics of the desired on-off gain mask.

III. Controller Architecture

In this section, given the Raman optimization tool description, a possible architecture of the autonomous Raman amplification module is outlined from an implementation point

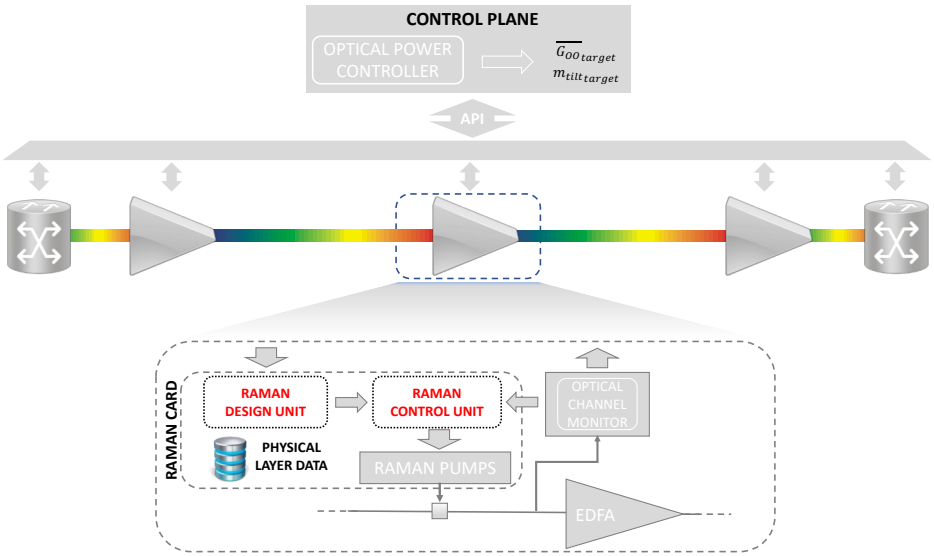

Fig. 2. Representation of the controller operation in a possible in-field implementation.

of view by defining the context of its operation in terms of interactions with the other modules (Fig. 2).

In the perspective of a SDN, we introduce the concept of a softwarized and autonomous Raman amplifier that is able to manage the Raman amplification per single fiber span, provided that only the amplification constraints are supplied. At the control plane level, the mean on-off gain and tilt targets (which define the needed Raman gain mask) are computed and transmitted via API to each Raman amplifier. In addition to Raman pumps, the Raman card has an on-board software module which is composed of two units: the Raman Design Unit (RDU) and the Raman Control Unit (RCU). The RDU receives the amplification constraints that are sent by the control plane and subsequently defines the optimal Raman pump power configuration, depending upon the physical layer parameters that are acquired during the initial probing of the equipment. These physical layer parameters include the fiber attenuation α, the Raman efficiency C_r and concentrated losses l_c. The RCU is responsible for setting the pump power levels according to the instructions given by the RDU and to exploit telemetry feedback, allowing the mean gain to be adjusted and the required target to be reached. Since the Raman design is carried out without considering the spectral load, the task of the RCU is to track the mean gain target. This task is fundamental, as the variable spectral load introduces a depletion effect between channels and pumps which has, as a consequence, an effective mean gain value that is lower than the designed one. This mean-gain compensation that is handled by the RCU is performed by linearizing the problem around the optimal working point. The optimal working point is provided by the RDU, by evaluating the gradient of each pump power level with respect to the on-off gain. Subsequently, the residual gap is divided proportionally according to the contribution given by each pump on the gain modification. The proposal of this Raman controller architecture is based on the possibility of having an appropriate computation power available on the Raman card. In this scenario, optical channel monitors (OCMs) allow autonomous requests of a design refinement from the RCU to the RDU in case of reasonable variations of the spectral load with respect to the calculated optimal working point. For example, the proposed architecture can suitably switch from single-band to multi-band transmission and vice versa. Moreover, in case of an inaccurate correspondence between the amplification target and the telemetry feedback due to the lack of information of the physical layer, the linear approximation around the optimal working point is able to maintain amplification constraints on a limited power interval, producing distortion of the on-off gain profile in terms of ripple and tilt. Remarkably, the described implementation can autonomously operate progressive improvements of the optimal working point, preventing this issue. Due to its flexibility and adaptation, the softwarization of the Raman amplification feature leads to the qualitative advantage that the system is able to promptly react to possible scenario modifications, such as fiber cuts and time degradation.

In the end, according to the features of the optical line system (in particular, the telemetry and the computational power of the on-board electronics), the Raman controller is able to assume different configurations depending upon the available resources.

IV. Experimental Campaign

In order to validate the potentiality of the developed design tool and to prove the efficiency of the delineated controller architecture, an experimental campaign has been carried out. In this section, the experimental equipment is described and we show all the steps performed to characterize the fiber, in order to acquire the physical layer data that is needed by the Raman amplification optimizer. Following this, we propose an experimental demonstration of the controller architecture be-

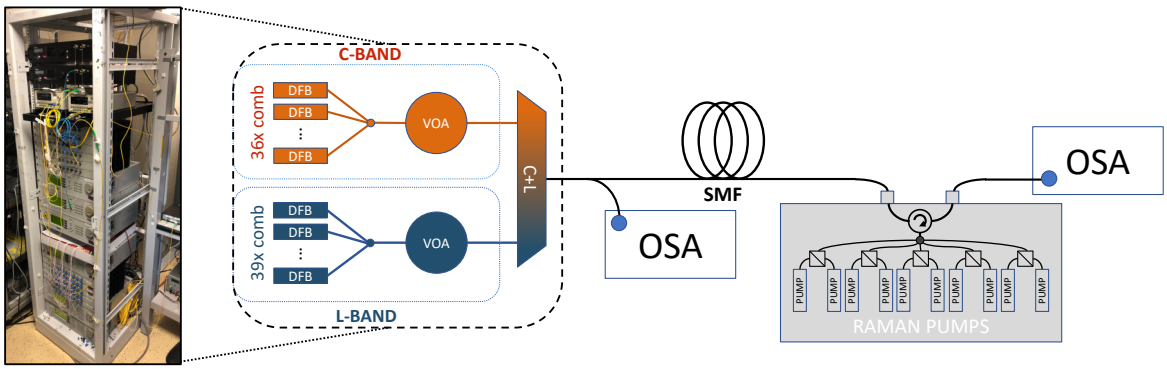

Fig. 3. Experimental setup built at the LINKS foundation photonic laboratory, Turin.

haviour, which emulates the operation of the software module in realistic working conditions.

A. Equipment Setup

The general scheme of the equipment setup is shown in Fig. 3. The input wavelength division multiplexing (WDM) spectrum is created by means of a system of polarized distributed feedback (DFB) lasers. Two different input WDM spectra are generated in L-band (39 channels) and C-band (36 channels), joining them into a single WDM spectrum using a C+L coupler. The power level of each DFB laser is tuned to obtain an almost flat spectrum around 0 dBm. Frequencies of DFB lasers are set in order to achieve standard 100 GHz C+L grid. Variable optical attenuators (VOA) are introduced to rigidly adjust C and L input spectra. A standard single mode fiber (SSMF) span with 85 km nominal length has been created joining two SSMF spools of 60 km and 25 km nominal lengths.

At the receiver side of the fiber span, a set of 5 counter-propagating Raman pumps with frequencies distributed in the range [200 - 210] THz is introduced by means of an optical circulator. The choice of the Raman pump frequency spectrum is made so that a suitable C+L multi-band transmission is enabled. Optical spectrum analysers (OSAs) are used to measure the WDM spectrum at both fiber span terminals.

B. Fiber Characterization

As first step, the fiber is characterized in order to acquire the physical layer information needed by the RDU for the optimization process. The fiber characterization is based on the measurement of the loss coefficient function α, the Raman efficiency C_r, and the concentrated losses distributed along the fiber span l_c. In this phase, a single fiber spool of 60 km nominal length is used to measure the loss coefficient function and the Raman efficiency with a higher degree accuracy . The entire C+L spectrum is swept using external-cavity lasers (ECLs).

The measured loss coefficient function is shown in Fig. 4. The power of a single ECL is measured for each frequency at the two terminations of the fiber spool. The loss coefficient function α is obtained by dividing the computed attenuation with the spool length at each frequency swept by the ECL.

A pump-and-probe system is adopted in order to evaluate

TABLE I
CONCENTRATED LOSSES

Loss Intensity	Loss Position
0.3 dB	0 km
0.2 dB	61.028 km
1.1 dB	86.102 km

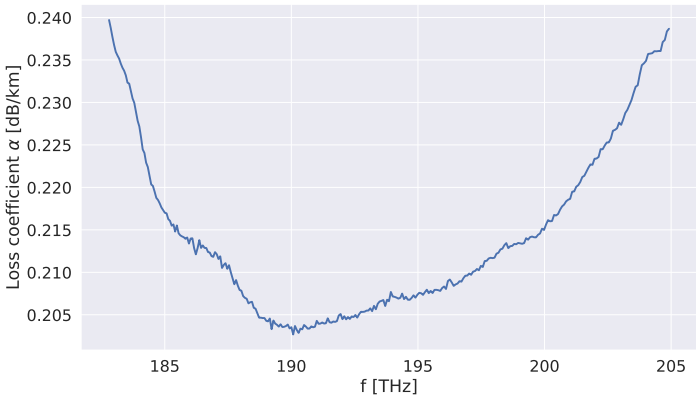

Fig. 4. Measured loss coefficient function.

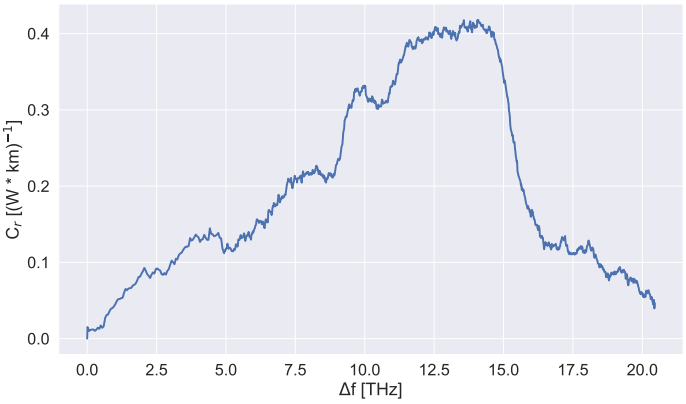

Fig. 5. Measured Raman Efficiency profile.

the Raman efficiency profile using a pair of ECLs (Fig. 5). The probe is a single polarization ECL with variable frequency and the pump is a depolarized ECL with fixed frequency which is higher than that of the probe. The power difference between the probe and the pump is fixed to approximately 20 dB, in order to ensure that the pump depletion is negligible. The Raman efficiency profile is computed according to the following formula [20]:

$$C_r(f_{ch}, f_p) = \frac{\ln\left(G_{OO}(f_{ch})\right)}{P(f_p, L_S) L_{eff}(f_p)} \tag{4}$$

where $P(f_p, L_S)$ is the pump launch power in linear units and $L_{eff}(f_p)$ is the effective length in meters, calculated as:

$$L_{eff}(f_p) = \frac{1 - e^{-\alpha(f_p) L_S}}{\alpha(f_p)} \tag{5}$$

In order to characterize the fiber span in terms of concentrated losses, the 60+25 km fiber span is subjected to an optical-time-domain reflectometer (OTDR) analysis. In addition, the circulator is properly characterized by focusing on the WDM spectrum and counter-propagating Raman pump paths. The summary of the intensity and the position of each concentrated loss is reported in Tab. I.

C. Experimental Demonstration

After having characterized the fiber span in terms of fiber properties and concentrated losses, an experimental demonstration of the developed software behaviour is presented.

The on-off gain $G_{OO}(f)$ is evaluated through the operative definition:

$$G_{OO}(f) = \frac{P_{S,ON}(f, L_S)}{P_{S,OFF}(f, L_S)} \tag{6}$$

where $P_{S,ON}(f, L_S)$ and $P_{S,OFF}(f, L_S)$ are the powers of a specific channel at the end of the fiber span with Raman pumps turned on and off, respectively.

Firstly, the WDM spectrum power profile is measured at both transmitter and receiver sides with Raman pumps turned off (Fig. 6). Starting from this measurement, we emulate the amplification constraints given by the control plane; the tilt target m_{target} is imposed as the linear regression slope of the measured spectrum power profile (Fig. 6-b) changed in sign, in order to completely rectify the amplified power spectrum. The mean on-off gain target $\overline{G_{OO,target}}$ is given as almost half of the attenuation introduced by the fiber span (8 dB). In this way, the below-transparency mode condition is ensured, avoiding NLI generation due to Raman amplification and a relevant part of the fiber attenuation is recovered. At this point, the RDU produces a configuration of Raman pump powers that matches the required amplification constraints and transmits it to the RCU, which is responsible for setting pump power levels. The optimal Raman pump power configuration is reported in Tab. II, where the first pump is at the highest frequency and the others are placed at lower decreasing frequencies.

From Fig. 7, the effect of the Raman pump configuration designed by the developed software module is visible. As expected, we observe that the on-off gain profile presents a mean value that is lower than that of the design due to the presence of the spectral load, which induces an emphasized depletion effect on each Raman pump power evolution. On the other hand, the optimization on the tilt appears to function adequately, correcting the power spectrum overall tilt by approximately one order of magnitude. In actuality, the spectrum tilt correction is substantial when referring to the C+L band, with the full-band tilt reducing to one tenth of the initial value of greater than 1 dB, producing a value which is very small with respect to the band in use. In order to correct the gap on the mean on-off gain, the RCU operates a linearization around the optimum working point defined by the RDU, attempting to raise the mean value of the on-off gain profile without changing either its shape or its tilt. This procedure should be performed in real-time with telemetry feedback until a certain tolerance that guarantees the maintenance of the on-

TABLE II
OPTIMAL RAMAN PUMP POWER CONFIGURATION

$P_{P,1}$	$P_{P,2}$	$P_{P,3}$	$P_{P,4}$	$P_{P,5}$
190.7 mW	150.9 mW	138.7 mW	34.7 mW	94.2 mW

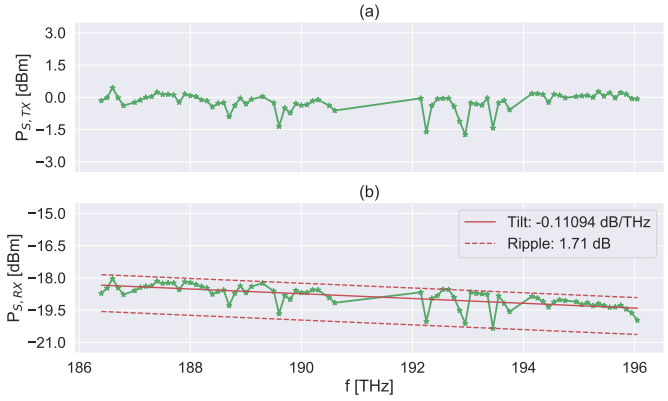

Fig. 6. Raman pumps off: (a) transmitted power spectrum, (b) received power spectrum.

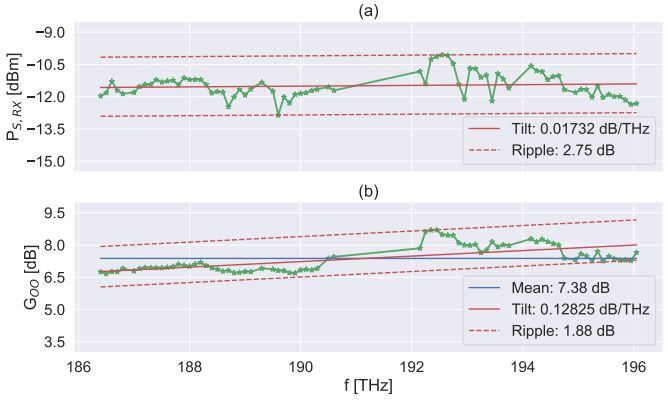

Fig. 7. Raman pumps on at the design power configuration: (a) received power spectrum, (b) on-off gain profile.

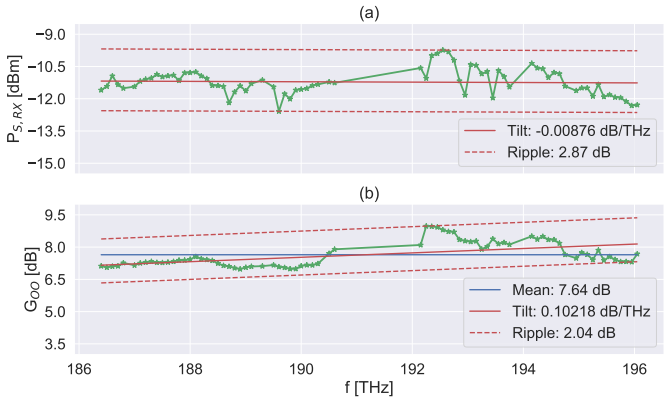

Fig. 8. Raman pumps at the compensated power configuration: (a) received power spectrum, (b) on-off gain profile.

TABLE III
COMPENSATED RAMAN PUMP POWER CONFIGURATION

$P_{P,1}$	$P_{P,2}$	$P_{P,3}$	$P_{P,4}$	$P_{P,5}$
201.5 mW	159.4 mW	146.5 mW	36.1 mW	99.5 mW

off gain tilt is reached. In this demonstration, we report the first computation made using the linear compensation in order to show the in-line operation of the software module. The compensated Raman pump power configuration is reported in Tab. III. From Fig. 8, improvement given by the linearization is observed. In particular, the increment of the mean on-off gain is evident: the gap with respect to the target value is reduced and the power spectrum tilt is preserved, continuing to be close to the no slope condition.

Finally, the on-off gain profile is designed to have the minimum possible ripple. Indeed, even if SRS tends to intrinsically twist the power spectrum profile, the ripple among channel remains contained within a range of 3 dB, showing in any case a homogeneity in the distribution of channel power peaks.

V. CONCLUSION

In this work, a numerical optimizer which addresses the problem of Raman amplification on a single fiber span for a specific SDN context is presented. The proposed controller architecture is able to autonomously handle Raman amplification, setting Raman pump power levels and interacting with devices present in a realistic in-field scenario. The operative behaviour and potentialities of this controller are demonstrated through an experimental campaign, highlighting the effective fulfillment of the expected objectives, and the quality and validity of the adopted physical model.

As a further improvement, starting from this approach, which tackles the problem in a pure analytical way, it is possible to integrate the optimization procedure by adopting machine-learning techniques; this would result in an improvement of the Raman amplification design quality and also the execution time of each phase of the in-field operation of the controller.

ACKNOWLEDGMENT

This work has been supported by Cisco Photonics within a SRA contract.

REFERENCES

[1] J. Bromage, "Raman amplification for fiber communications systems," *Journal of Lightwave Technology*, vol. 22, no. 2, p. 79, 2004.

[2] K. Rottwitt and A. J. Stentz, "Raman amplification in lightwave communication systems," in *Optical Fiber Telecommunications IV-A*. Elsevier, 2002, pp. 213–257.

[3] M. N. Islam, "Raman amplifiers for telecommunications," *IEEE Journal of selected topics in Quantum Electronics*, vol. 8, no. 1, pp. 548–559, 2002.

[4] M. Cantono, A. Ferrari, D. Pilori, E. Virgillito, J. Augé, and V. Curri, "Physical layer performance of multi-band optical line systems using raman amplification," *Journal of Optical Communications and Networking*, vol. 11, no. 1, pp. A103–A110, 2019.

[5] P. Hansen, L. Eskildsen, S. Grubb, A. Stentz, T. Strasser, J. Judkins, J. DeMarco, R. Pedrazzani, and D. DiGiovanni, "Capacity upgrades of transmission systems by raman amplification," *IEEE Photonics Technology Letters*, vol. 9, no. 2, pp. 262–264, 1997.

[6] L. E. Nelson, B. Zhu, L. Leng, J. Bromage, and H.-J. Thiele, "High-capacity, raman-amplified long-haul transmission and the impact of optical fiber properties," in *Optical Transmission Systems and Equipment for WDM Networking II*, vol. 5247. International Society for Optics and Photonics, 2003, pp. 26–39.

[7] A. Ferrari, D. Pilori, E. Virgillito, and V. Curri, "Power control strategies in c+l optical line systems," in *Optical Fiber Communication Conference*. Optical Society of America, 2019, pp. W2A–48.

[8] A. Carena, V. Curri, and P. Poggiolini, "On the optimization of hybrid raman/erbium-doped fiber amplifiers," *IEEE Photonics Technology Letters*, vol. 13, no. 11, pp. 1170–1172, 2001.

[9] V. Curri and A. Carena, "Merit of raman pumping in uniform and uncompensated links supporting nywdm transmission," *Journal of Lightwave Technology*, vol. 34, no. 2, pp. 554–565, 2015.

[10] P. Hansen, A. Stentz, T. Nielsen, R. Espindola, L. Nelson, and A. Abramov, "Dense wavelength-division multiplexed transmission in "zero-dispersion" dsf by means of hybrid raman/erbium-doped fiber amplifiers," in *Optical Fiber Communication Conference*. Optical Society of America, 1999, p. PD8.

[11] S. Namiki and Y. Emori, "Ultrabroad-band raman amplifiers pumped and gain-equalized by wavelength-division-multiplexed high-power laser diodes," *IEEE Journal of Selected Topics in Quantum Electronics*, vol. 7, no. 1, pp. 3–16, 2001.

[12] V. E. Perlin and H. G. Winful, "Optimal design of flat-gain wide-band fiber raman amplifiers," *Journal of lightwave technology*, vol. 20, no. 2, p. 250, 2002.

[13] ——, "On distributed raman amplification for ultrabroad-band long-haul wdm systems," *Journal of lightwave technology*, vol. 20, no. 3, p. 409, 2002.

[14] Y. Li and D. C. Kilper, "Optical physical layer sdn," *Journal of Optical Communications and Networking*, vol. 10, no. 1, pp. A110–A121, 2018.

[15] T. J. Xia, H. Fevrier, T. Wang, and T. Morioka, "Introduction of spectrally and spatially flexible optical networks," *IEEE Communications Magazine*, vol. 53, no. 2, pp. 24–33, 2015.

[16] X. Zhao, V. Vusirikala, B. Koley, V. Kamalov, and T. Hofmeister, "The prospect of inter-data-center optical networks," *IEEE Communications Magazine*, vol. 51, no. 9, pp. 32–38, 2013.

[17] J. Oliveira, J. Oliveira, M. Siqueira, R. Scaraficci, M. Salvador, L. Mariote, N. Guerrero, L. Carvalho, F. van't Hooft, G. Santos *et al.*, "Towards software defined autonomic terabit optical networks," in *Optical Fiber Communication Conference*. Optical Society of America, 2014, pp. M3H–5.

[18] V. Curri, A. Carena, P. Poggiolini, G. Bosco, and F. Forghieri, "Extension and validation of the gn model for non-linear interference to uncompensated links using raman amplification," *Optics express*, vol. 21, no. 3, pp. 3308–3317, 2013.

[19] ScipyCommunity. (2018-2019) Scipy. [Online]. Available: https://docs.scipy.org/doc/scipy/reference/index.html

[20] E. Pincemin, D. Grot, L. Bathany, S. Gosselin, M. Joindot, S. Bordais, Y. Jaouen, and J.-M. Delavaux, "Raman gain efficiencies of modern terrestrial transmission fibers in s-, c-and l-band," in *Nonlinear Guided Waves and Their Applications*. Optical Society of America, 2002, p. NLTuC2.